Pharm Res (2013) 30:131–139
DOI 10.1007/s11095-012-0855-9

RESEARCH PAPER

Influence of Process Conditions on the Crystallization and Transition of Metastable Mannitol Forms in Protein Formulations During Lyophilization

Wenjin Cao • Yong Xie • Sampathkumar Krishnan • Hong Lin • Margaret Ricci

Received: 25 May 2012 / Accepted: 2 August 2012 / Published online: 21 August 2012

ABSTRACT

Purpose To study the impact of different process conditions and formulation compositions on metastable mannitol forms in protein formulations during lyophilization.

Methods Mannitol was studied with and without other formulation components. A cryostage was used to mimic the different processing steps during lyophilization. The different mannitol forms were monitored and quantified with an *in situ* Raman spectroscopic method. In addition, a Raman imaging method was developed to characterize the spatial distribution of mannitol forms in final lyophilization samples from the freeze-drying stage.

Results Amorphous mannitol was observed during fast cooling (10°C/min) and with the addition of other formulation component. Amorphous mannitol crystallized into mainly δ and hemihydrate forms during annealing at −20°C. Under vacuum without moisture, dried amorphous mannitol could transform to mainly α form at 45°C and greater. The transformation mechanism of the hemihydrate mannitol was similar to that of amorphous form.

Conclusion Mannitol tends to crystallize into stable crystalline forms by itself, but the addition of lyoprotectant (e.g. sucrose) and protein helps stabilize the metastable forms (hemihydrate and amorphous). The metastable forms are capable of transforming into mixtures of different forms, with heat and moisture being the critical processing factors.

KEY WORDS lyophilization · mannitol · metastable · Raman · Raman imaging

INTRODUCTION

Mannitol is a commonly used excipient in lyophilized protein formulations. Its high eutectic temperature with ice allows for the use of higher primary drying temperature, which results in good cake properties and short lyophilization cycle. However, since the protein resides in the amorphous phase, mannitol crystallized during lyophilization leads to less protein protection (1,2). As a result, mannitol is usually used in combination with other lyoprotectants in protein formulations (3,4).

Mannitol has five known solid-state forms, three anhydrous forms (5), two metastable forms, a hemihydrate (6–8) and amorphous form (9–11). The metastable mannitol forms are known to transform to anhydrous forms during the lyophilization process (6–11) and storage (6–8) and they have significant impact on the quality of lyophilized products (1,2,7,8,12–15). Amorphous mannitol can lose its protein stabilizing effects when it crystallizes (1,2). Izutsu reported enzyme inactivation and non-covalent aggregation

W. Cao (✉) • M. Ricci
Department of Drug Product Development, Amgen Inc.
One Amgen Center Dr., M/S 8-2-D
Thousand Oaks, California 91320, USA
e-mail: wcao@amgen.com

Y. Xie
Analytical R&D, Amgen Inc.
Thousand Oaks, California, USA

S. Krishnan
Global Biologics R&D, Hospira Inc.
Lake Forest, Illinois, USA

H. Lin
Small Molecule Pharmaceutical Sciences, Genentech
South San Francisco, California, USA

due to amorphous mannitol crystallization during annealing (1). Hemihydrate mannitol poses more stability challenges as it can release water upon heating and during storage even at room temperature (8) or below (7). Water is known to facilitate solid-state degradation either as a plasticizer to reduce the glass transition temperature (Tg), and thus increase molecular mobility, or as a reactant in many chemical reactions, such as hydrolysis and deamidation (12). The adverse impact of water on lyophilized protein products is well documented in the literature, e.g. aggregation (13), deamidation (4), Asp isomerization (14), and oxidation (15). The metastable mannitol forms are the major sources of variability observed in lyophilized products, and are very sensitive to formulation and process parameters. There is a need for better understanding of both metastable forms, amorphous and hemihydrate, in order to deliver a mannitol-containing lyophilized formulation with the desired product quality profile.

Given the wide use of mannitol in lyophilization formulations, extensive characterization has been done to understand the physical forms of mannitol during lyophilization (1,3,6–11,16,17) with the majority of the work focusing on the crystallization of mannitol and limited studies on the transformations of metastable mannitol forms (18). This is due to both the limitations of the analytics and the instability of metastable forms. In the published studies, various techniques have been used to characterize the different mannitol forms, such as XRPD (9,16), DSC (10,17), TGA (7), Near IR (8), FT-IR (5) and Raman (19). However, none of them was able to characterize and quantify all five forms (especially amorphous and hemihydrate) simultaneously during the lyophilization process. A recent method was developed in our lab to quantify all five mannitol forms using Raman spectroscopy during *in situ* monitoring (20). The method, with quantitation limits ranging from ±3% for pure mannitol forms and ±5% for lyophilized protein samples, enables us to understand the transformation of metastable mannitol forms during lyophilization. Here we focus on studying the impact of formulation and processing parameters on the crystallization and transformation of two metastable mannitol forms, the hemihydrate and amorphous form. Because of their unstable nature, the metastable forms are likely to have multiple transition pathways and can transform to different anhydrous forms under different process conditions. Understanding of their transformation pathways could provide better process control and reduce batch-to-batch variations.

The Development of Raman Imaging Method

Raman imaging technology has become an increasingly utilized characterization technique for the pharmaceutical and biotechnology industry (21). Various imaging techniques have been developed with Raman, including point-by-point scanning (21), line scanning (22) and focal plane imaging such as the application of LCTF in ChemImage Raman system (23). Compared with the focus plane imaging technique, the point-by-point scanning method utilizes dispersive Raman for collecting the signal, which is slower than the focus plane imaging technique. However, for the application of studying lyophilized protein, the normal advantages of the focal plane imaging technique are not applicable, where the studied material has a chemical distribution in millimeter scale, and samples need large Raman shift window and long integration for a dramatic fluorescent background change and less distinct Raman signals. The point-by-point scanning technique is able to handle these requirements, which are common in pharmaceutical applications. In this study, we use a point scanning montage method to collect Raman signal for constructing Raman images in a 7 mm × 7 mm area with a step size of 245 μm to study the heterogeneous distribution of mannitol polymorphs within samples.

MATERIALS AND METHODS

Materials

The experiments were done on three types of formulations: 1) mannitol only; 2) mannitol with sucrose and Tris (hydroxymethyl)aminomethane buffer; and 3) mannitol, sucrose, Tris buffer and protein. The mannitol concentration was 4% (*w/v*) in all the studies. Other excipients included 1% sucrose and 10 mM Tris buffer at pH 7.4. The protein concentrations studied were 20 and 50 mg/mL.

All chemicals and solvents used were reagent grade or better. The model fusion protein used in the study was produced by recombinant technologies in Chinese Hamster Ovary cells and purified by processes proprietary to Amgen (Seattle, WA, USA).

Methods

Raman Instrument

All the Raman spectra were obtained using a FALCON II™ Molecular Chemical Imaging (MCI) system from ChemImage Corporation (Pittsburgh, PA, USA). The excitation source was the Millennia II I Laser Source (Spectra Physics, Mountain View, CA, USA) at 532 nm, coupled with a Model BX51 microscope platform (Olympus, Center Valley, PA, USA). The Raman spectra were collected with a 20× objective from a sample area of ca. 154 μm. A back illuminated CCD (Princeton Instruments, Trenton, NJ, USA) with 1340 × 100 pixels was used as detector for Raman signals.

Real-Time Monitoring of Mannitol Forms Using Quantitative Raman Spectroscopy Method

A freeze-drying cryostage, able to simulate the freeze drying process (FDCS 196 from Linkam Scientific Instruments Ltd., Tadworth, Surrey, UK), was customized to couple with the Raman microscope system to collect Raman spectra during lyophilization. This cryostage has a temperature control from −196°C to 125°C, and pressure control from 50 mTorr to 750 Torr. About 5 μL of sample solution was placed between two circular sapphire windows (support: 22 mm, cover: 7 mm) and placed inside the cryostage. Samples were monitored during the lyophilization process in real-time with Raman spectroscopy *in situ* through the glass window of the cryostage. For the freezing study, the sample solution was first cooled to −50°C with varying cooling rate. Samples were then held at −50°C for about 8 min before heating at 1°C/min to −20°C for the annealing step. After annealing at −20°C for 30 min, samples was cooled to −50°C and held for 10 min under vacuum at100 mTorr. Samples were then heated at 1°C/min to −20°C and dried at that temperature. For the drying study, samples were subjected to vacuum at various temperatures to study the combined effects of temperature and moisture on mannitol transformation during drying. Raman spectra were typically taken on samples every 5°C when the temperature changed or every 5 min when the temperature was held constant to monitor mannitol crystallization during the freezing. The Raman spectra were processed using the developed method to quantify the different forms (20).

X-ray Powder Diffractometry

The X-ray powder diffraction (XRPD) analysis was performed using a θ/θ diffractometer (X'pert MPD, Philips Analytical, Natick, MA) with Cu Kα radiation. All samples were analyzed with Bragg-Brentano geometry from 3-40° 2θ at a step size of 0.01° 2θ.

Raman Imaging

The Raman imaging experiments were conducted on lyophilized samples formed between two circular sapphire windows. The cover and support windows were 7 mm and 22 mm in diameters, respectively. About 5 μL of sample solution was placed between the two windows, pressed to remove any air bubbles, and then lyophilized. For the Raman imaging study, a 7 mm×7 mm square area was scanned to cover the entire sample area with step size of 245 μm. A Raman image contained 900 (30×30) individual dispersive Raman spectra. The image data were first classified using a PLS classification method to differentiate sapphire-signal-only data from data contain mannitol information. Then the MCR quantitation method (20) was used to predict the percentage of 5 mannitol forms for each imaging data. For imaging data processing, a narrow Raman shift window was used from 1010 cm^{-1} to 1550 cm^{-1} to avoid the sapphire interference. Once the predicted percentages of each form were calculated for each imaging data, the imaging data were reconstructed to a false-color image by using a color panel to define the percentages range from 0 to 100%. The color images illustrate the spatial distributions of different mannitol forms within samples.

RESULTS AND DISCUSSION

Crystallization During Freezing (Cooling Rate, Annealing, and Formulation)

Crystallization of mannitol during the freezing step was first studied with respect to cooling rate in the absence of other formulation components. Figure 1 shows the plot of predicted percentage of mannitol forms *vs.* time by *in situ* Raman spectroscopic monitoring. With a cooling rate of 1°C/min (Fig. 1a and b), mannitol directly crystallized into primarily β and δ mannitol. The example in Fig. 1a showed crystallization into mainly the δ form, whereas in another run (Fig. 1b) the majority crystallized into β mannitol. The run-to-run difference was suspected due to a heterogeneous spatial distribution of mannitol forms from a slow-cooling crystallization. Data were taken from multiple spots of the same samples (data not shown) and the *in situ* Raman imaging study shown in the later section clearly provided evidence of a heterogeneous distribution of mannitol forms crystallized under slow cooling rate. Therefore, Raman spectra were taken from multiple spots on the final freeze-dried samples to characterize the distribution and average out the differences.

For the fast cooling rate (10°C/min), crystallization of mannitol from solution was inhibited and resulted in amorphous mannitol when the solution was cooled down to −50°C (Fig. 1c). Amorphous mannitol, when subjected to annealing at −20°C, most of the amorphous form crystallized into mainly δ and some hemihydrate form. The result showed that amorphous mannitol started to crystallize into primarily the δ form at temperature around −25°C. Our observation under varying cooling rates was consistent with the published literature (10,11).

Besides processing parameters, formulation components are also known to impact mannitol crystallization (3,9,10,16,17). Mannitol in different formulations can manifest in different crystallization behavior, as described in introduction. In this study, four types of mannitol formulations were tested to understand the individual contributions

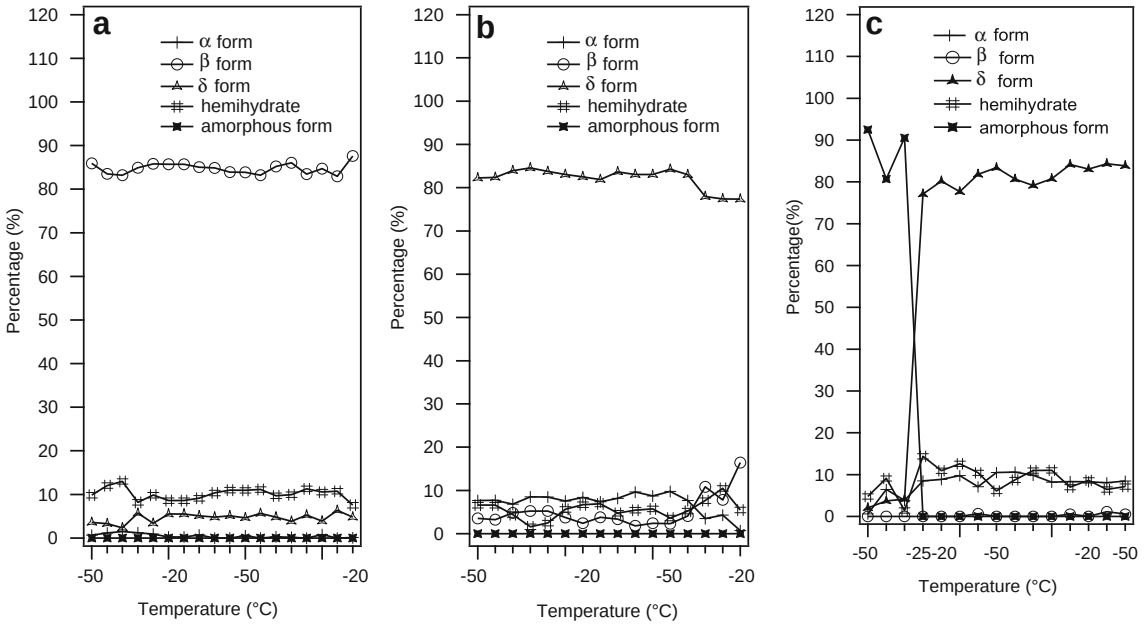

Fig. 1 Mannitol crystallized into mainly β and δ forms with (**a** and **b**) slow cooling (1°C/min, replicate runs) and (**c**) fast cooling (10°C/min). The fast cooling sample was annealed at −20°C.

of multiple formulation factors on mannitol crystallization: 4% mannitol solution, 4% mannitol with 1% sucrose, 4% mannitol with 1% sucrose and 10 mM Tris–HCl buffer at pH 7.4 (TMS buffer), and mannitol in protein formulations that include different protein concentrations (20 mg/mL and 50 mg/mL) in TMS buffer.

As mentioned in the previous section, pure mannitol solution directly crystallized to crystalline β and δ when subjected to cooling rates of 1°C/min. However, with the presence of other formulation components, such as sucrose and/or protein, mannitol crystallization was delayed or prohibited even at a slow cooling rate (1°C/min), as shown in Figs. 2 and 3. Figure 2 shows the crystallization of the TMS buffer sample at a cooling rate of 1°C/min. The study on the TMS buffer samples showed mannitol solidified into mainly the amorphous form at 1°C/min cooling rate and transformed into primarily the δ form and some hemihydrate upon annealing at −20°C. The crystallization of samples that contained 4% mannitol and 1% sucrose was similar to that of TMS buffer.

The addition of protein to the formulation had a direct impact on the transformation pathways of mannitol. Two protein formulation samples (20 mg/mL and 50 mg/mL) were cooled to −50°C at 1°C/min and annealed at −20°C. With the present of protein, the data showed at least two effects on mannitol crystallization. First, increased protein concentrations resulted in a delay in the crystallization of amorphous mannitol during annealing. Secondly, higher protein concentrations caused more amorphous mannitol to transform to the hemihydrate form. As shown in Fig. 3, mannitol crystallization was observed within samples after annealing for 10 min at 20 mg/mL, and 20 min for samples at 50 mg/mL. Also, the asterisks in Fig. 3 indicated the Raman features correlated to mannitol hemihydrate. Mannitol hemihydrate was of special interest in this study because its physical instability and potential detrimental effects on the lyophilized drug product. Based on these results, the hypothesized crystallization pathway for mannitol hemihydrate is through amorphous mannitol, and protein concentration has a positive correlation to the amount of mannitol hemihydrate crystallizes in formulations.

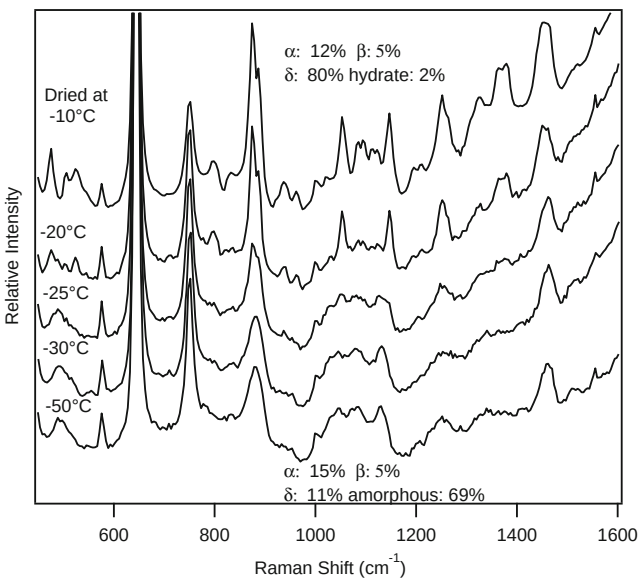

Fig. 2 Mannitol in the TMS buffer solidified into mainly the amorphous form at 1°C/min cooling rate. It subsequently transformed to primarily the δ form and some hemihydrate upon annealing at −20°C.

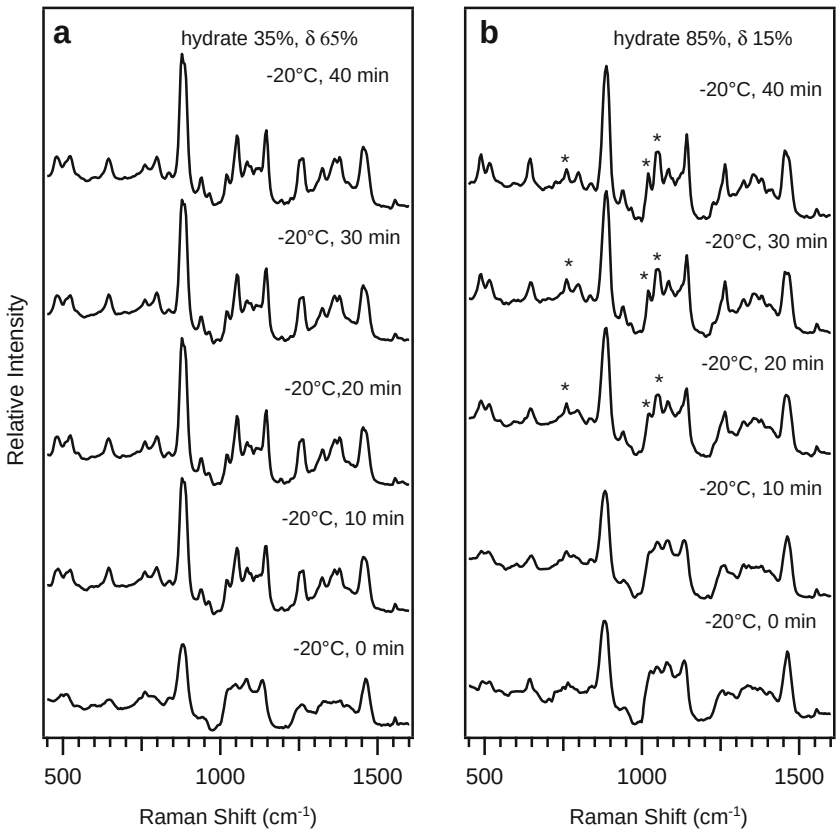

Fig. 3 The *in situ* Raman monitoring of (**a**) 20 mg/mL and (**b**) 50 mg/mL protein formulations during the −20°C annealing process. The asterisks indicate the existence of high percentage of mannitol hemihydrate.

Transformation During Drying (Drying Temperature and Moisture Impact)

Transformation of metastable mannitol forms (e.g. amorphous and hemihydrate mannitol) are expected during primary and secondary drying stages with the presence of heat and moisture. This study revealed several transition routes for those two forms, which have potential impact on the final product quality.

Amorphous mannitol usually formed during fast cooling or with high sucrose and/or high protein concentration in the formulation. Amorphous mannitol was known to be unstable (9,24,25). Literature has reported that amorphous mannitol was difficult to characterize because of its instability and fast transformation. Even at sub-ambient temperature, it could transform into other stable forms in a short time (24). In the previous section, amorphous mannitol was found to be a key form in both crystallization and transformation pathways of mannitol containing formulations at sub-ambient temperatures. This study focused on a systematic understanding of transformation pathways of amorphous mannitol at different drying conditions with *in situ* real time monitoring.

As shown in the previous freezing and annealing section, amorphous mannitol crystallized around −25°C during annealing into mainly δ and hemihydrate form at sub-ambient temperature. Moreover, the annealing products from amorphous mannitol were consistent regardless of the formulation components. Higher protein concentrations, however, favored the formation of higher amounts of mannitol hemihydrate.

The impact of drying parameters on the transformation of amorphous mannitol was of interest because not all amorphous mannitol crystallizes during annealing. Current studies found that amorphous mannitol underwent different transformation pathways during drying than those at annealing. In one study, amorphous mannitol was first dried at −35°C for an hour and then heated to 25°C under vacuum. The amorphous mannitol sample remained stable at 25°C for at least an hour. Once vacuum was released, amorphous mannitol immediately transformed into a mixture of β and δ mannitol at 25°C. The XRPD data on the final forms also confirmed this transition of amorphous mannitol. Figure 4 showed the Raman data for these two transformations. Figure 4a is the Raman spectrum when amorphous mannitol was annealed around −25°C into mainly δ and hemihydrate form and Fig. 4b is the Raman spectrum of the final forms crystallized from dried amorphous mannitol at 25°C after exposure to moisture. The mannitol forms were primarily β and δ forms.

Dried amorphous mannitol, if subjected to a high temperature as experienced in some aggressive secondary drying

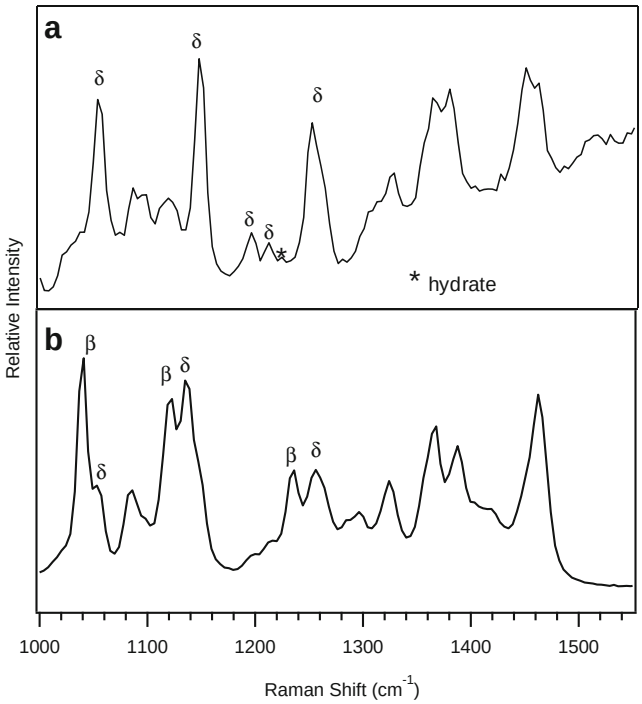

Fig. 4 The Raman spectra taken from the crystallization product of amorphous mannitol after (**a**) annealing at −20°C and (**b**) exposing to moisture at 25°C after being completely dried at −35°C. The asterisks mark mannitol hemihydrate peaks.

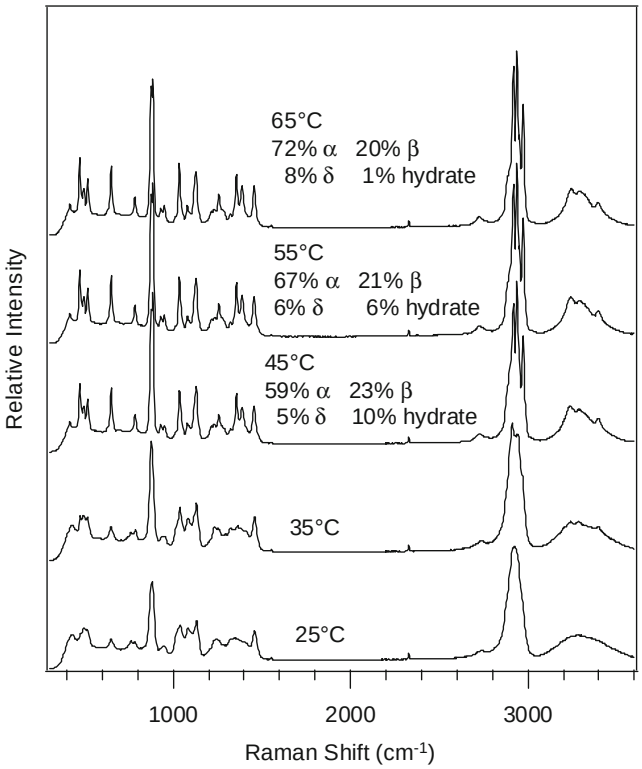

Fig. 5 The temperature-dependent *in situ* Raman monitoring for the thermal transition of dried amorphous mannitol under 100 mTorr vacuum.

cycles, undergoes yet another transformation pathway revealed by *in situ* Raman monitoring. In Fig. 5, dried amorphous mannitol displayed a Raman spectrum having a typical broad and smooth band at around the 2800 cm^{-1} region at 25°C. As the temperature increased to 35°C under vacuum, some sharp features were observed in a region that overlapped with this broad C-H stretch Raman band. At temperatures above 45°C, a significant spectral change was observed. Further analysis by the quantitation method showed that α mannitol was the main form generated under 45°C drying conditions.

The three different transition routes of amorphous mannitol could explain the observations of potentially inconsistent distributions of mannitol forms amongst different batches and even amongst vials from same batch. Even with constant processing parameters, the local variances, such as the temperature gradient inside the lyophilizer or the different drying efficiency associated with a large quantity of samples, could have an impact on the amorphous mannitol within the formulation and the subsequent transformation to different mannitol forms.

Mannitol hemihydrate was another metastable mannitol form that could transform under lyophilization conditions. For hemihydrate mannitol, similar transformation patterns were observed as for amorphous mannitol. At ambient conditions without vacuum, hemihydrate mannitol slowly dehydrated into mostly β and some δ mannitol forms. The transformation of hemihydrate mannitol during the freeze-drying process was followed as a function of temperature by Raman in-process monitoring (Fig. 6). Similar to what was observed in the drying of amorphous mannitol, hemihydrate mannitol dehydrated into primarily the α mannitol form at a temperature higher than 45°C under vacuum.

Formulation samples with higher protein concentration contained a relatively large amount of mannitol hemihydrate after the annealing step. After being subjected to the same drying cycle as utilized for the placebo formulations, the protein-containing samples also showed significant amounts of α form of mannitol. This result was consistent with the observation of the transition from pure mannitol hemihydrate to mainly α mannitol at temperature above 45°C. However, less α mannitol was present in the final product for protein-containing samples compared to pure mannitol placebo samples, (29% *vs.* 64%, respectively). Moreover, the sample with 20 mg/mL protein concentration showed overall less hemihydrate after annealing and thus less α form after drying compared to the 50 mg/mL samples.

In summary, formulation components, such as sucrose and protein, inhibited mannitol crystallization so the direct crystallization of mannitol from freezing was limited and mannitol stayed as an amorphous form. Amorphous mannitol, after annealing, crystallized into mainly the δ form.

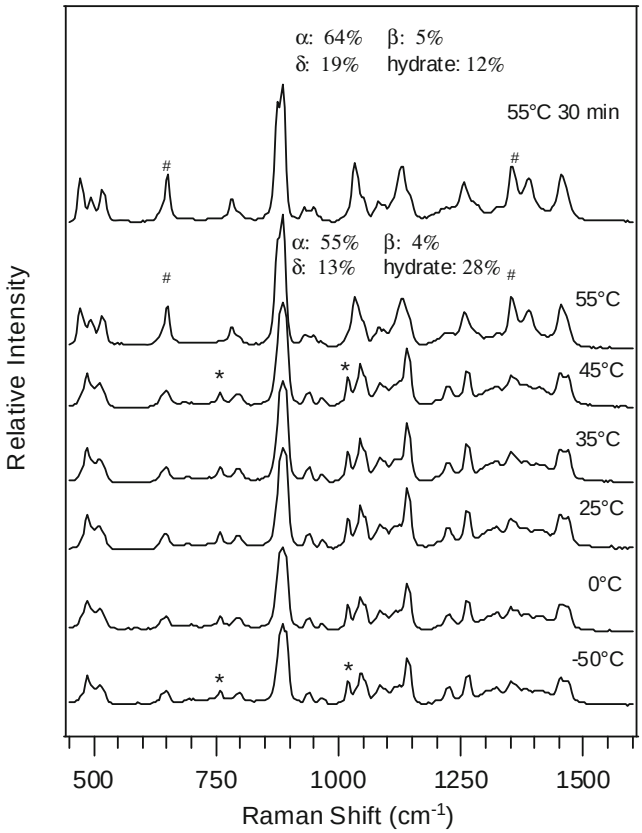

Fig. 6 The temperature-dependent *in situ* Raman monitoring for the thermal dehydration process of mannitol hemihydrate under 100 mTorr vacuum condition. The asterisks mark mannitol hemihydrate peaks; and # marks α mannitol peaks.

However, protein seemed to stabilize the hemihydrate form and the high protein concentration formulation resulted in more hemihydrate formation. Amorphous and hemihydrate mannitol, if dried, was stable under vacuum at room temperature and underwent transition to α form at temperatures equal to or above 45°C. However, these two metastable forms were sensitive to the combination of moisture and temperature. They transformed to mainly the β and δ forms at room temperature with moisture.

Raman Imaging for Distribution of Mannitol Polymorphs in Lyophilized Samples

Raman imaging data were able to provide chemical structure information in lyophilization products at a broader scale compared to the limited sampling area of *in situ* Raman monitoring. Raman image data shown in Fig. 7 were obtained on final lyophilized products from 4% mannitol placebo solution under different cooling rates.

The *in situ* data had shown that the slow cooling rate of 1°C/min resulted in the direct crystallization of mannitol from the solution phase. However, as shown in Fig. 1, the crystallization results were not consistent from run to run, as some samples were rich in δ mannitol while others were mainly β mannitol. One possible explanation was the heterogeneous distribution of crystallization products within each sample, and that our real-time observation was

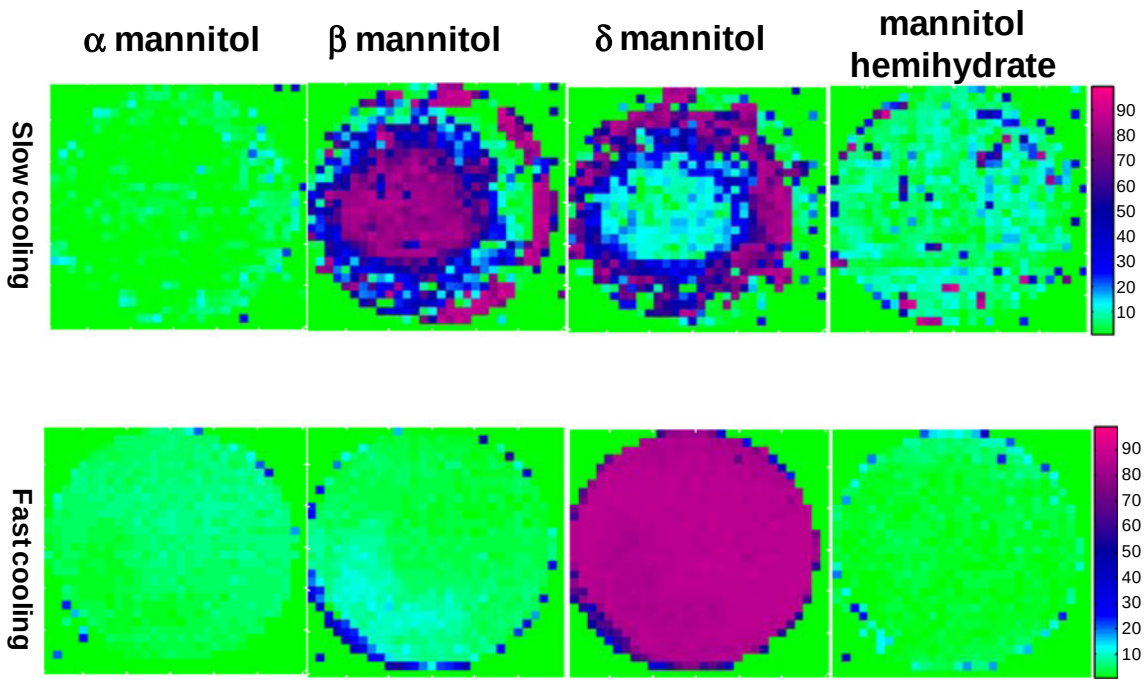

Fig. 7 The Raman images of the lyophilized mannitol samples from 5 μL of 4% mannitol solution with different cooling rate controls of 1°C/min for the top four images and 10°C/min for the bottom four images. The Raman images are organized in the order of α, β, δ, and hemihydrate forms from left to right for both top and bottom rows.

confined to a 154 μm diameter sample area which was not representative of the whole sample. The imaging data confirmed this hypothesis. The top four Raman images in Fig. 7 showed the distribution of α, β, δ, hemihydrate mannitol in a sample crystallized using a lyophilization cycle with a 1° C/min cooling rate. The Raman images showed that the main polymorphs from direct crystallization of slow cooling were β and δ forms, with the δ form located more on the edge and the β form more in the center of this lyophilized product. The bottom four Raman images were from a sample generated with a 10°C/min fast cooling rate and annealing. The imaging of the fast cooling sample was consistent with the observation from *in situ* monitoring, showing δ mannitol as the main annealing product. The latter fast-cooling process, which formed amorphous mannitol during freezing and induced crystallization by annealing, generated more consistent polymorphs and more uniform distributions, suggesting this might be a more controlled crystallization process than slow cooling for 4% mannitol solutions.

The same experiment was performed on 5 μL TMS buffer solution. Due to the inclusion of 1% sucrose, the fast and slow cooling rates resulted in similar outcomes. Both samples crystallized through amorphous mannitol, and their Raman images were similar to what was observed in Fig. 7b.

CONCLUSION

Mannitol crystallization was highly sensitive to the formulation composition and the lyophilization cycle processing parameters, resulting in a combination of different physical forms of mannitol with unique properties. Mannitol tended to crystallize into stable forms in mannitol-only placebo formulations, but the addition of lyoprotectant (e.g. sucrose) and protein induced the metastable forms (e.g. hemihydrate and amorphous forms). The drying temperature and moisture were found to have significant effects on the transformation behavior of the metastable forms and resulted in multiple combinations of mannitol forms.

The results observed on the *in situ* Raman freeze-drying microscope system helped elucidate the various transition pathways of amorphous and hemihydrate mannitol, which could potentially be the source of the batch-to-batch and even vial-to-vial variability of mannitol forms in the lyophilized product. An understanding of the crystallization and transformation pathways of metastable mannitol forms is an essential prerequisite to design a robust lyophilized protein formulation and lyophilization process.

In addition to providing a mechanistic understanding of mannitol transformational pathways, these studies also showed the utility of the Raman imaging method to quantitatively characterize the heterogeneous distribution of mannitol crystallization products. The wide range of Raman imaging information was complementary to *in situ* Raman monitoring data from a limited sample area. This technique was especially insightful for samples with a heterogeneous distribution of crystallization products, for which inconsistent observations by *in situ* monitoring could be elucidated by whole sample Raman imaging.

ACKNOWLEDGMENTS AND DISCLOSURES

The authors thank Nina Cauchon for discussion and the summer intern program at Amgen Inc. for funding.

REFERENCES

1. Izutsu K, Yoshioka S, Terao T. Decreased protein-stabilizing effects of cryoprotectants due to crystallization. Pharm Res. 1993;10(8):1232–7.
2. Izutsu K, Yoshioka S, Terao T. Effect of mannitol crystallinity on the stabilization of enzymes during freeze-drying. Chem Pharm Bull. 1994;42(1):5–8.
3. Johnson RE, Kirchhoff CF, Gaud HT. Mannitol-sucrose mixtures-versatile formulations for protein lyophilization. J Pharm Sci. 2002;91(4):914–22.
4. Cleland JL, Lam X, Kendrick B, Yang J, Yang T, Overcashier D, *et al.* A specific molar ratio of stabilizer to protein is required for storage stability of a lyophilized monoclonal antibody. J Pharm Sci. 2001;90(3):310–21.
5. Burger A, Henck JO, Hetz S, Rollinger JM, Weissnicht AA, Stottner H. Energy/temperature diagram and compression behavior of the polymorphs of D-mannitol. J Pharm Sci. 2000;89(4):457–68.
6. Yu L, Milton N, Groleau EG, Mishra DS, Vansickle RE. Existence of a mannitol hydrate during freeze-drying and practical implications. J Pharm Sci. 1999;88(2):196–8.
7. Nunes C, Suryanarayanan R, Botez C, Stephens PW. Characterization and crystal structure of D-mannitol hemihydrate. J Pharm Sci. 2004;93 (11):2800–9.
8. Cao W, Mao C, Chen W, Lin H, Krishnan S, Cauchon N. Differentiation and quantitative determination of surface and hydrate water in lyophilized mannitol using NIR spectroscopy. J Pharm Sci. 2006;95(9):2077–86.
9. Kim AI, Akers MJ, Nail SL. The physical state of mannitol after freeze-drying: effects of mannitol concentration, freezing rate, and a noncrystallizing cosolute. J Pharm Sci. 1998;87(8):931–5.
10. Telang C, Yu L, Suryanarayanan R. Effective inhibition of mannitol crystallization in frozen solutions by sodium chloride. Pharm Res. 2003;20(4):660–7.
11. Cavatur RK, Vemuri NM, Pyne A, Chrzan Z, Toledo-Velasquez D, Suryanarayanan R. Crystallization behavior of mannitol in frozen aqueous solutions. Pharm Res. 2002;19(6):894–900.
12. Shalaev EY, Zografi G. How does residual water affect the solid-state degradation of drugs in the amorphous state? J Pharm Sci. 1996;85(11):1137–41.
13. Liu WR, Langer R, Klibanov M. Moisture-induced aggregation of lyophilized proteins in the solid state. Biotechnol Bioeng. 1991;37:177–84.
14. Breen ED, Curley JG, Overcashier DE, Hsu CC, Shire SJ. Effect of moisture on the stability of a lyophilized humanized monoclonal antibody formulation. Pharm Res. 2001;18(9):1345–53.
15. Pikal MJ, Dellerman K, Roy ML. Formulation and stability of freeze-dried proteins: effects of moisture and oxygen on the stability

of freeze-dried formulations of human growth hormone. Dev Biol Standard. 1991;74:21–38.
16. Dixon D, Tchessalov S, Barry A, Warne N. The impact of protein concentration on mannitol and sodium chloride crystallinity and polymorphism upon lyophilization. J Pharm Sci. 2009;98(9):3419–29.
17. Liao X, Krishnamurthy R, Suryanarayanan R. Influence of the active pharmaceutical ingredient concentration on the physical state of mannitol -implications in freeze-drying. Pharm Res. 2005;22(11):1978–85.
18. Liao X, Krishnamurthy R, Suryanarayanan R. Influence of processing conditions on the physical state of mannitol-implications in freeze-drying. Pharm Res. 2007;24(2):370–6.
19. Beattie JR, Barrett LJ, Malone JF, McGarvey JJ, Nieuwenhuyzen M, Kett VL. Investigation into the subambient behavior of aqueous mannitol solutions using temeprature-controlled Raman microscopy. Eur J Pharm Biopharm. 2007;67(2):569–78.
20. Xie Y, Cao W, Krishnan S, Lin H, Cauchon N. Characterization of mannitol polymorphic forms in lyophilized protein formulations using a Multivariate Curve Resoultion (MCR)-based Raman spectroscopic method. Pharm Res. 2008;25 (10):2292–301.
21. Bhargava R, Schaeberle MD, Levin IW. Raman and mid-infrared microspectroscopic imaging. In: Braiman MS, Gregoriou VG, editors. Vibrational spectroscopy of biological and polymeric materials. CRC Press; 2006. p. 215–52.
22. Markwort L, Kip B. Micro-Raman imaging of heterogeneous polymer systems: general applications and limitations. J Appl Polym Sci. 1996;61(2):231–54.
23. Turner II JF, Treado PJ. LCTF Raman chemical imaging in the near-infrared. Proc SPIE. 1997;3061:280–3.
24. Cavatur RK, Suryanarayanan R. Characterization of phase transitions during freeze-drying by *in situ* X-ray powder diffractometry. Pharm Dev Technol. 1998;3(4):579–86.
25. Yu L, Mishra DS, Rigsbee DR. Determination of the glass properties of D-mannitol using sorbitol as an impurity. J Pharm Sci. 1998;87(6):774–7.